Enhanced Nucleation Fields due to Dipolar Interactions in Nanocomposite Magnets

Johann Fischbacher*, Simon Bance, Lukas Exl, Markus Gusenbauer,
Harald Oezelt, Franz Reichel and Thomas Schrefl
St. Poelten University of Applied Sciences
Matthias Corvinus-Strasse 15
3100 St. Poelten, Austria †

Abstract

One approach to construct powerful permanent magnets while using less rare-earth elements is to combine a hard magnetic material having a high coercive field with a soft magnetic material having a high saturation magnetization at the nanometer scale and create so-called nanocomposite magnets. If both materials are strongly coupled exchange forces will form a stable magnet. We use finite element micromagnetics simulations to investigate the changing hysteresis properties for varying arrays of soft magnetic spherical inclusions in a hard magnetic body. We show that the anisotropy arising from dipolar interactions between soft magnetic particles in a hard magnetic matrix can enhance the nucleation field by more than 10 % and strongly depends on the arrangement of the inclusions.

1 Introduction

Most high performance magnets today are based on rare-earth elements like neodymium or dysprosium. These are both expensive and in short supply. One approach to construct even more powerful permanent magnets while using less rare-earth elements is to combine two different magnetic alloys at the nanometer scale and create so-called *nanocomposite* or *exchange spring* magnets. The idea behind this is to combine a hard magnetic material having a high coercive field with a soft magnetic material having a high saturation magnetization. If the coercive field of a magnet is high enough, its energy density product is proportional to the magnetization squared. If both materials of a nanocomposite magnet are strongly coupled, exchange forces will form a stable magnet with energy products as high as 1 MJ/m^3, with low rare-earth content [1, 2].

The enhancement of the remanence and the energy density product is generally achieved at the expense of the coercivity. But exchange interactions between soft and hard magnetic phases preserve a high coercivity if the size of the magnetically soft region is smaller than twice the domain wall width of the hard magnetic phase [3].

To obtain a significant enhancement of the energy density product it is necessary to include a large amount of soft phase within the hard magnetic matrix. But if the distance between neighboring soft inclusions becomes too small, i.e. the thickness of the hard region is less than the domain wall width δ, the soft regions interact and the nucleation field is reduced significantly. The nucleation field is independent of the shape of the soft region as long as its size is small enough [2]. Skomski and Coey [2] showed that the nucleation field of nanocomposite structures is given by $2\langle K\rangle/(\mu_0\langle M\rangle)$, where $\langle K\rangle$ is the volume averaged anisotropy constant and $\langle M\rangle$ is the volume averaged magnetization. Thus the nucleation field decreases with increasing volume fraction of soft magnetic phases.

But high-magnetization materials can be used to create shape anisotropy. Therefore nanoscale magnetostatic self-interactions may increase the energy product while the volume fraction of the magnetic phase decreases. This effect is exploited in alnico magnets consisting of FeCo needles in an AlNi matrix [4]. Skomski et al. [4] found a maximum energy product $(BH)_{max} = \mu_0 M_r^2/12$ for such magnets where M_r is the remanence and the volume fraction of the hard phase $f = 2/3$. In this work we

*Johann.Fischbacher@fhstp.ac.at

†Submitted to The European Physical Journal B, published online 18 March 2013, Eur. Phys. J. B. (2013) 86: 100, DOI: 10.1140/epjb/e2013-30938-1. The original publication is available at http://epjb.epj.org/articles/epjb/abs/2013/03/b120938/b120938.html

will look at the optimal arrangement of soft nano-spheres embedded in a hard magnetic matrix. Similar to the shape anisotropy of needles, the dipolar interactions between nano-spheres may increase the coercive field.

Hadjipanayis and co-workers [1] proposed to build exchange spring permanent magnets with a bottom-up approach from nano-sized magnetic particles. After compaction a hard magnetic matrix with soft magnetic inclusions will be formed. Since the soft particles have a higher magnetization than the hard magnetic matrix, dipolar interactions between the soft inclusions will influence the magnetic behavior. It is well known that magnetic anisotropy can arise from magnetic dipoles arranged in a lattice [5, 6]. The magnetic field outside a magnetized sphere is similar to a magnetic dipole field. In a theoretical model of a nanocomposite magnet, we can assume that the soft inclusions are spheres. Thus dipolar interactions may lead to an additional effective anisotropy that can enhance the coercive field.

In this work we investigate the effect of dipolar interaction between the soft inclusions in nanocomposite permanent magnets. We assume soft magnetic spheres that are distributed in a hard magnetic matrix phase and use finite element micromagnetics simulations to compute the coercive fields for different arrangements of the spheres within the hard matrix. The results show, that dipolar interactions between the soft inclusions can stabilize the magnet. Remarkably, it is possible to enhance the coercive field although the volume fraction of the soft magnetic phase is increased.

2 Method

We use finite element micromagnetics to compute the magnetization reversal of our models. Micromagnetism is a continuum theory describing magnetization processes on a characteristic length scale of a few nanometers. We solve the Gilbert equation given by

$$\frac{\partial \vec{M}}{\partial t} = -|\gamma| \vec{M} \times \vec{H}_{\text{eff}} + \frac{\alpha}{M_s} \vec{M} \times \frac{\partial \vec{M}}{\partial t} \quad (1)$$

$$\vec{H}_{\text{eff}} = \vec{H}_{\text{E}} + \vec{H}_{\text{A}} + \vec{H}_{\text{M}} + \vec{H}_{\text{ext}} \quad (2)$$

for a time varying external field. Details of the numerical implementation are given in [7]. First the external field is kept zero for 10 ns, in order obtain the remanent magnetic state. Then the external field, $\mu_0 H_{ext}$ is decreased to -6 T with a slope of -0.12 T/ns. In order to introduce a symmetry breaking, the field is applied at an angle of 0.5 degrees with respect to the easy direction of the hard magnetic phase. The Gilbert damping constant α is one. Equation (1) describes the motion of the magnetization $\vec{M}$ in the effective field $\vec{H}_{\text{eff}}$. It is the sum of the exchange field $\vec{H}_{\text{E}}$, the anisotropy field $\vec{H}_{\text{A}}$, the magnetostatic or dipolar field $\vec{H}_{\text{M}}$, and the applied external field $\vec{H}_{\text{ext}}$.

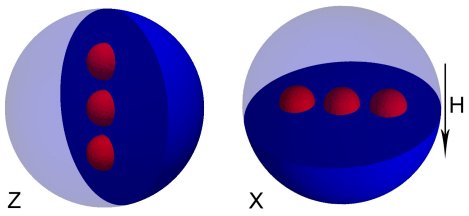

Figure 1: Small $Fe_{65}Co_{35}$ spheres placed inside a $Nd_2Fe_{14}B$ body.

We use $Nd_2Fe_{14}B$ with uniaxial anisotropy constant $K_1 = 4.9 \times 10^6$ J/m^3, magnetic polarization $J_s = 1.61$ T and exchange constant $A = 7.7 \times 10^{-12}$ J/m. For the simulations we assume a weak uniaxial anisotropy in the soft magnetic phase of $K_1 = 4.0 \times 10^4$ J/m^3, a magnetic polarization of $J_s = 2.43$ T ($Fe_{65}Co_{35}$) and exchange constant of $A = 2.6 \times 10^{-11}$ J/m. The anisotropy axes of the soft and the hard magnetic phases are parallel.

We place an array of soft magnetic spheres oriented along the x-axis or z-axis as shown in Fig. 1 in a hard magnetic matrix ($Nd_2Fe_{14}B$) and apply an external field in z-direction with the easy axis of the magnetic materials in the same direction as the external field. The hard magnetic matrix has the form of a sphere. Thus we can avoid any effects of the macroscopic shape. Furthermore the macroscopic demagnetizing field is uniform for a sphere. Simulations of which the results are compared with each other are done with a constant diameter d_{shell} of the $Nd_2Fe_{14}B$ matrix phase. In general d_{shell} is held as small as possible to keep the number of finite elements low.

3 Results

In a first set of simulations we investigate the influence of the size of the soft magnetic inclusions on the reversal process. We place three small soft magnetic spheres inside a hard magnetic shell. In one case the inclusions are arranged along the x-axis, in the second they are arranged along the z-

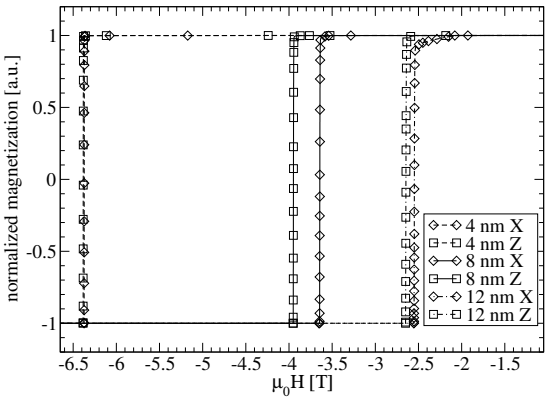

Figure 2: Magnetic reversal of three soft magnetic spheres with $d_{incl} = 4, 8, 12$ nm in a hard magnetic matrix of constant diameter $d_{shell} = 48$ nm. The labels X and Z refer to the arrangement of the inclusions along the x-axis or z-axis, respectively. The external field $\mu_0 H$ is applied in z-direction. The easy axis of the magnetic materials is parallel to the z-direction.

axis. In both cases an external field $H_{ext} = \mu_0 H$ is applied in z-direction. The diameter d_{incl} of the $Fe_{65}Co_{35}$ spheres is incremented from 4 nm up to 14 nm with a gap of 1 nm inbetween them. The diameter d_{shell} of the $Nd_2Fe_{14}B$ shell is 48 nm. Any difference in the nucleation field between the vertical arrangement of the soft spheres and the horizontal arrangement of the soft spheres has to be attributed to dipolar interactions between the soft inclusions. Fig. 2 shows the resulting hysteresis curves and Table 1 the differences in the nucleation fields. The effect due to dipolar interaction is strongest for inclusions with $d_{incl} = 8$ nm. We observe a 8.4 % higher nucleation field when the soft magnetic spheres are aligned parallel to the direction of the applied external field as compared to the case when the soft magnetic spheres are aligned perpendicular to H_{ext}. For diameters $d_{incl} = 4$ nm and $d_{incl} = 14$ nm the effect vanishes which is due to the very strong or the very weak exchange hardening of the soft phase, respectively. For proper exchange hardening the size of the inclusions should not be more than twice the domain wall width of $Nd_2Fe_{14}B$ given by $\delta = \pi\sqrt{A/K_1} \approx 3.94$ nm, where K_1 is the uniaxial anisotropy constant and A is the exchange constant [3]. Note that with growing amount of $Fe_{65}Co_{35}$ in the system the coercive field diminishes.

In a second set of computations we investigate the effect of a shrinking gap between the soft magnetic inclusions. We place three soft magnetic

Table 1: Nucleation fields for a system of three soft magnetic spherical inclusions in a hard magnetic matrix of diameter $d_{shell} = 48$ nm. The size of the inclusions is changed from $d_{incl} = 4, \ldots, 14$ nm. The labels X and Z reference to the alignment of the inclusions along the x-axis or z-axis, respectively. The external field $\mu_0 H$ is applied in z-direction. We assume $\mu_0 H_{nuc}$ when the normalized magnetization reaches 0.8.

d_{incl}	$\mu_0 H^x_{nuc}$[T]	$\mu_0 H^z_{nuc}$[T]	$\frac{\mu_0 H^z_{nuc} - \mu_0 H^x_{nuc}}{\mu_0 H^x_{nuc}}$
4 nm	-6.3706	-6.3798	0.14 %
6 nm	-4.7569	-5.0048	5.21 %
8 nm	-3.6396	-3.9454	8.40 %
10 nm	-2.9795	-3.1799	6.72 %
12 nm	-2.5424	-2.6399	3.83 %
14 nm	-2.2297	-2.2419	0.55 %

spheres with $d_{incl} = 8$ nm in a hard magnetic body with $d_{shell} = 42$ nm, again arranged along the x-axis in one case and along the z-axis in the second one. H_{ext} is applied in z-direction. The gap between the soft magnetic inclusions is varied from 0.5 nm to 5 nm. The coercive field is reduced with shrinking gap as predicted in [2]. But the effect due to dipolar interactions is getting larger when the gap is getting smaller as shown in Table 2. While we notice a difference of just 3.46 % between $\mu_0 H^z_{nuc}$ and $\mu_0 H^x_{nuc}$ when the distance between the inclusions is 5 nm, this difference rises to 10 % for a gap of 0.5 nm. $\mu_0 H^z_{nuc}$ and $\mu_0 H^x_{nuc}$ denote the nucleation field for the vertical arrangement of the soft spheres and the horizontal arrangement of the soft spheres, respectively. What's remarkable is that $\mu_0 H^z_{nuc}$ of the models with a gap of 0.5 nm or 1 nm between the soft particles is comparable to $\mu_0 H^x_{nuc}$ for the model with a gap of 5 nm. If the soft inclusions are arranged in chains parallel the easy axis of the matrix phase, the dipolar interaction is obviously reinforcing the $Fe_{65}Co_{35}$ spheres, additionally to the exchange coupling with the $Nd_2Fe_{14}B$ shell.

The magnetic reversal is shown in Fig. 3. Considering the reversal dynamics of the model with the inclusions arranged parallel to the x-axis, we notice that the strayfields of the two outside spheres act on the central sphere and force it to nucleate first. For the model with the soft magnetic balls arranged vertically (in the direction the external field and the easy direction of the hard matrix), we expect a reinforcement of the central sphere by the two outside spheres. This can be observed for gaps

Table 2: Nucleation field of three soft magnetic spheres ($d_{incl} = 8$ nm) inside a hard magnetic shell ($d_{shell} = 42$ nm). The gap between the inclusions is varied from 0.5 nm to 5 nm. The labels x and z comply with the alignment of the soft magnetic balls along the x-axis or along the z-axis, respectively. The external field is applied in z-direction. $\mu_0 H_{nuc}$ is the value of the external field when a normalized magnetization 0.9 is reached.

gap	$\mu_0 H^x_{nuc}$[T]	$\mu_0 H^z_{nuc}$[T]	$\frac{\mu_0 H^z_{nuc} - \mu_0 H^x_{nuc}}{\mu_0 H^x_{nuc}}$
0.5 nm	-3.6014	-3.9615	10.00 %
1.0 nm	-3.6945	-4.0416	9.40 %
2.0 nm	-3.8470	-4.1303	7.36 %
3.0 nm	-3.9602	-4.1895	5.79 %
4.0 nm	-4.0446	-4.2299	4.58 %
5.0 nm	-4.0953	-4.2369	3.46 %

of 4 nm or larger. But for smaller gaps a stronger demagnetizing field of the $Nd_2Fe_{14}B$ matrix (the hard phase with holes for the soft inclusions) in the location of the central inclusions is competing with the dipolar reinforcement and therefore is forcing it to nucleate first.

Next we increase the amount of $Fe_{65}Co_{35}$ in our models and investigate what happens if we have longer chains of soft magnetic inclusions in the $Nd_2Fe_{14}B$ matrix. Fig. 4 shows the magnetic reversal for 3, 5 and 7 spheres with $d_{incl} = 8$ nm arranged in one line along the x- or z-axis with H_{ext} applied again in z-direction. Remarkable is that if the soft magnetic spheres are arranged parallel to the external field then due to dipolar interactions the nucleation field stays approximately the same (only 0.5 % difference) while the volume of soft magnetic inclusions is more than doubling. But if those spheres are aligned perpendicular to H_{ext} the additional $Fe_{65}Co_{35}$ is decreasing the coercive field significantly. In Table 3 we see differences of up to 15.46 % in $\mu_0 H_{nuc}$ for those alignments, depending on the number of soft magnetic inclusions and the gap between them. Again a smaller gap results in bigger effect due to dipolar interaction but a slightly smaller coercive field due to a different demagnetizing field and exchange hardening potential. Regarding the magnetic reversal process the observations mentioned before for small gaps are again valid. Nucleation starts at the central sphere and then moves outwards pairwise, i.e. first the central sphere, then its two next neighbors, followed by their next neighbors and so on.

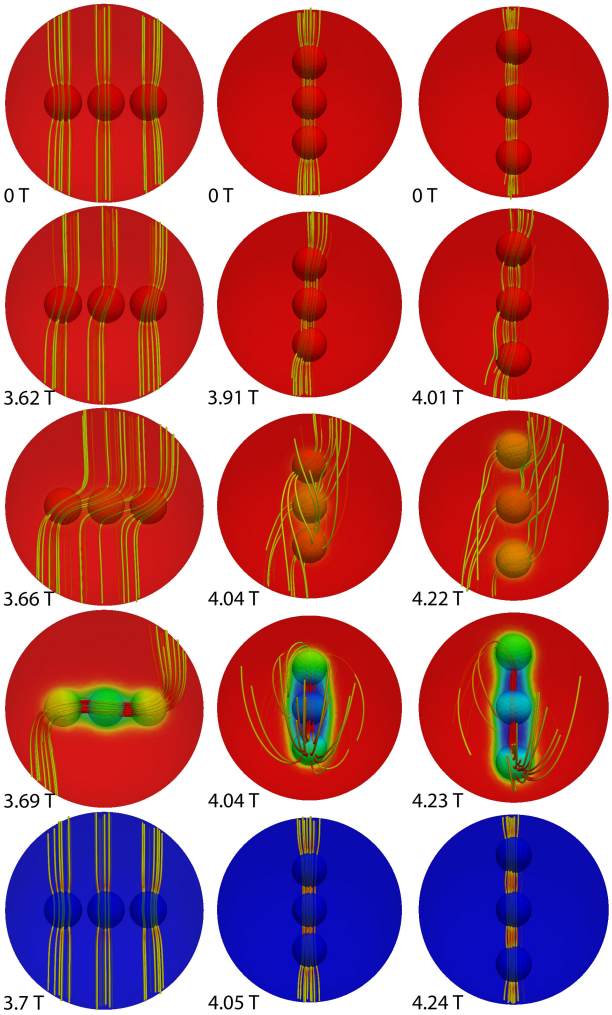

Figure 3: Magnetic reversal process: The pictures show the magnetic flux lines. The color denotes the magnetization direction (red: magnetization up, blue magnetization down). The gap between the soft magnetic spheres ($d_{incl} = 8$ nm) is 1 nm in the first two columns and 4 nm in the third column. The external field is applied in z-direction and its value is written next to each picture. In the first column the soft magnetic inclusions are aligned perpendicular to the applied external field. The interaction with the outside inclusions is weakening the central sphere and forces it to switch first. In the second and third column the soft magnetic spheres are aligned in a parallel manner to the applied external field. The two outside spheres reinforce the central one and therefore nucleation should not start in the center. But for gaps smaller than 4 nm a strong demagnetizing field in the location of the central sphere caused by the shell diminishes the strengthening effect due to dipolar interaction.

Table 3: Nucleation field of 3/5/7 soft magnetic spheres (d_{incl} = 8 nm) in a hard magnetic matrix (d_{shell} = 72 nm). The gap between the inclusions is varying from 0.5 nm to 2 nm. Longer chains of soft magnetic spheres decrease the coercive field significantly if aligned perpendicular to the applied external field but keep the coercive field constant in the other case. The labels X and Z refer to the alignment of the inclusions along the x-axis or z-axis, respectively. The external field is applied in z-direction. $\mu_0 H_{nuc}$ is the value of the external field when the normalized magnetization is 0.9.

gap	spheres	$\mu_0 H^x_{nuc}$[T]	$\mu_0 H^z_{nuc}$[T]	$\frac{\mu_0 H^z_{nuc} - \mu_0 H^x_{nuc}}{\mu_0 H^x_{nuc}}$
0.5 nm	3	-3.5978	-3.9492	9.77 %
	5	-3.4552	-3.9299	13.74 %
	7	-3.4034	-3.9297	15.46 %
1.0 nm	3	-3.7029	-4.0478	9.31 %
	5	-3.5650	-4.0395	13.31 %
	7	-3.5082	-4.0367	15.06 %
2.0 nm	3	-3.8536	-4.1372	7.39 %
	5	-3.7466	-4.1458	10.65 %
	7	-3.7088	-4.1382	11.58 %

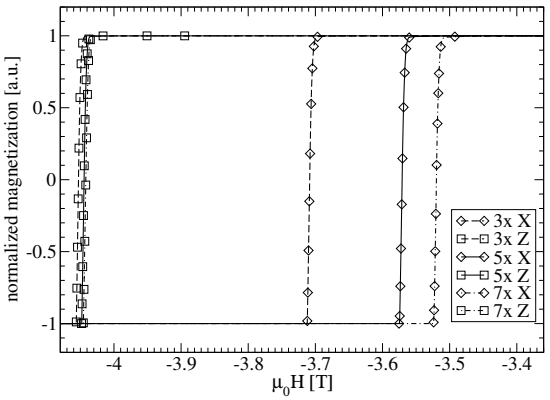

Figure 4: Magnetic reversal of 3/5/7 soft magnetic spheres (d_{incl} = 8 nm) in a hard magnetic matrix (d_{shell} = 72 nm). The reinforcement due to dipolar interaction is capable of eliminating the expected reduction of the coercive field due to the extra $Fe_{65}Co_{35}$ in the model if the inclusions are aligned in a parallel manner to the applied external field. The labels X and Z refer to the alignment of the inclusions along the x-axis or z-axis, respectively. The external field is applied in z-direction. The easy axis of the hard magnetic matrix is parallel to the z-direction.

So far the $Fe_{65}Co_{35}$ spheres in our models have been arranged perfectly inline. In the next set of simulations we place three spheres of size $d_{incl} = 8$ nm along the z-axis and then translate the central sphere along the y-axis to introduce non-perfect chains. This imperfection in the arrangement of the spheres is measured with an angle β which is defined as the angle between the z-axis and a straight line between the centers of the lower and the translated central sphere. As the problem is not symmetric anymore the resulting model is rotated so that we get the three orientations x, y and z as shown in Fig. 5 and apply H_{ext} in z direction. The spheres are translated in a way that the gap is kept constant at 1 nm while β is rising. $d_{shell} = 42$ nm.

In general the introduction of some deviation from the perfect inline model is decreasing the maximum possible coercive field as shown in Fig. 6. But for any angle β one of the three models shown in Fig. 5 is outperforming the other two. Therefore there are possibilities to fit many chains of soft magnetic inclusions next to each other without decreasing the coercive field too much.

When having a closer look on the magnetic reversal process we see that the central sphere is interacting mainly with one of its neighbors and neglecting the other one. This is different to the inline model where all three spheres are interacting. If we reconsider Fig. 3 showing the reversal of some inline models, we see the fieldlines passing through all three spheres. But with rising β the fieldlines passing through the translated central sphere and one of

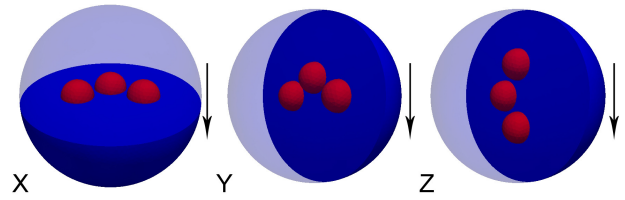

Figure 5: Introducing some deviation from the in-line models used before. The central sphere is translated to open a misarrangement angle β between the respective system axis and a straight line through the centers of one of the outside spheres and the translated central sphere. The position of the outside soft magnetic inclusions is adapted to keep the gap between the sphere constant at 1 nm for all β. The arrows show the orientation of the applied external field.

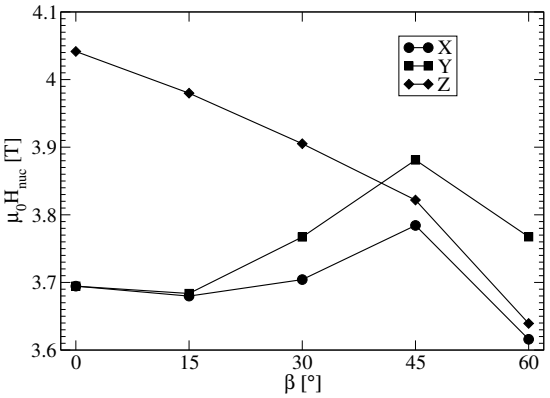

Figure 6: $\mu_0 H_{nuc}$ for different β. The labels X, Y and Z match the models as shown in Fig. 5. There is always one orientation outperforming the two others. $\mu_0 H_{nuc}$ is the value of the external field when the normalized magnetization in the demagnetization curves drops below 0.9.

its neighbors cannot bend to also pass through the third inclusion and therefore reduces the intensity of interaction.

In the next simulations we place multiple chains of $Fe_{65}Co_{35}$ inclusions next to each other as shown in Fig. 7.

In a first approach we arrange the soft magnetic particles (d_{incl} = 8 nm) in a $3 \times 3 \times 3/5/7$ lattice with a gap of 1 nm inbetween them as shown on the right-hand side of Fig. 7. The diameter of the hard magnetic body is 76 nm. If 63 soft magnetic spheres are placed inside that shell the model consists of approximately 7.4 vol.% $Fe_{65}Co_{35}$ and 92.6 vol.% $Nd_2Fe_{14}B$. In the case of 27 inclusions the model contains approx. 3.3 vol.% $Fe_{65}Co_{35}$.

When the soft magnetic chains are arranged perpendicular to the easy axis of the hard matrix we observe a decreasing coercive field as more $Fe_{65}Co_{35}$ is placed inside the $Nd_2Fe_{14}B$ body as shown in Fig. 8. But when the chains are arranged parallel to the easy axis the opposite is happening and the magnet with the higher $Fe_{65}Co_{35}$ share is performing better in terms of coercivity. The share of $Fe_{65}Co_{35}$ in the magnet is increased by approximately 240 % when placing 63 inclusions instead of 27 into the $Nd_2Fe_{14}B$ body and still $\mu_0 H^z_{nuc}$ of the magnet with 63 soft magnetic particles is 0.7 % higher.

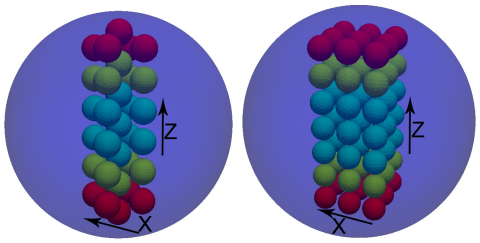

Figure 7: Soft magnetic spheres (d_{incl} = 8 nm) in a hard magnetic body. The different shadings of the inclusions refer to the varying number of spheres used for computing the magnetic reversal. The left model is used to compute the reversal for 11, 21 and 31 inclusions aligned in 5 chains of spheres where two spheres of the central chain and its common neighbor in an outside chain form an equilateral triangle (see also Fig. 6, $\beta = 60°$). For the right model the spheres are aligned in a $3 \times 3 \times 3/5/7$ lattice. The gap between the spheres is in both cases 1 nm and the external field and the easy directions are parallel to the x or z direction pictured by those arrows.

In a second arrangement shown on the left-hand side of Fig. 7 we shift the outside chains with respect to the central chain in a way that two central spheres and their common outside neighbor are arranged in an equilateral triangle. For a misarrangement angle $\beta = 60°$, $\mu_0 H_{nuc}$ is reduced significantly for any orientation of the applied external field as shown in Fig. 6. Still, due to dipolar interactions, even when almost tripling the number of soft magnetic inclusions the loss in coercivity can be neglected, as shown in Fig. 9.

4 Conclusions

In nanocomposite magnets dipolar interactions between the soft inclusions might be used to stabilize the coercive field. The influence of an effective anisotropy induced by dipolar interactions has been

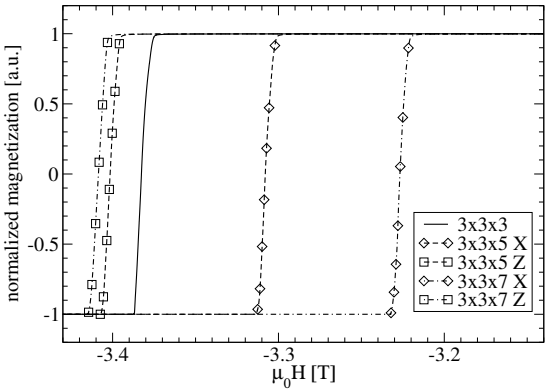

Figure 8: Magnetic reversal of a $Nd_2Fe_{14}B$ sphere filled with 27/45/63 $Fe_{65}Co_{35}$ inclusions arranged as shown on the right-hand side of Fig. 7. The labels X and Z refer to the orientation of the applied external field. Remarkable is the gain of coercive field although the amount of $Fe_{65}Co_{35}$ is increased and the amount of $Nd_2Fe_{14}B$ is decreased.

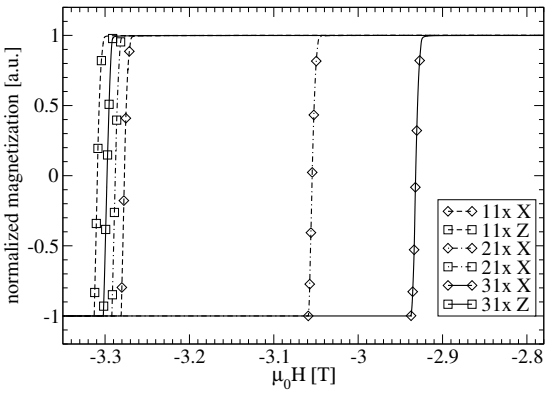

Figure 9: Magnetic reversal of a $Nd_2Fe_{14}B$ sphere filled with 11/21/31 $Fe_{65}Co_{35}$ inclusions arranged as shown on the left-hand side of Fig. 7. The labels X and Z refer to the orientation of the applied external field and the easy directions. Although we almost triple the number of $Fe_{65}Co_{35}$ inclusions the resulting coercive field stays approximately the same if the orientation of the model is chosen the right way.

shown for soft magnetic spheres embedded in a hard magnetic matrix. Micromagnetic simulations show that the coercive field can be altered by up to 15 percent by rearranging the soft magnetic spheres while the volume fraction between the hard and the soft phases is kept the same.

References

[1] Hadjipanayis, G. and Gabay, A., IEEE Spectrum **48**(8), (2011) 36–41.

[2] Skomski, R. and Coey, J. M. D., Am. Physical Soc. Phys. Rev. B **48**, (1993) 15812–15816.

[3] Schrefl, T., Kronmüller, H. and Fidler, J., J. Magn. Magn. Mater. **127**, (1993) L273–L277.

[4] Skomski, R., Liu, Y., Shield, J. E., Hadjipanayis, G. C. and Sellmyer, D. J., J. Appl. Phys. **107**, (2010) 09A739-1–09A739-3.

[5] Mizoguchi, T. and Cargill III, G. S., J. Appl. Phys. **50**, (1979) 3570–3582.

[6] Cohen, M. H. and Keffer, F., Phys. Rev. **99**, (1955) 1128–1134.

[7] Schrefl, T., Hrkac, G., Bance, S., Suess, D., Ertl, O. and Fidler, J., Numerical Methods in Micromagnetics (Finite Element Method), *Handbook of Magnetism and Advanced Magnetic Materials* **2**(John Wiley & Sons, Ltd., 2007).